Aerobiologia (2014) 30:239–255
DOI 10.1007/s10453-013-9324-0

ORIGINAL PAPER

Analysis of atmospheric dispersion of olive pollen in southern Spain using SILAM and HYSPLIT models

M. A. Hernandez-Ceballos · J. Soares · H. García-Mozo · M. Sofiev · J. P. Bolivar · C. Galán

Received: 16 October 2012 / Accepted: 4 December 2013 / Published online: 12 December 2013

Abstract SILAM atmospheric dispersion model and the HYSPLIT trajectory model were used to detect the source areas and calculate transport dynamics for airborne olive pollen observed in the city of Córdoba, southwest of Iberian Peninsula. The ECMWF weather data with 3-h time interval and spatial resolution of 25×25 km^2 and 75 hybrid vertical levels were used as meteorological inputs in both models to produce a coherent set of results in order to compare these two different approaches. Seven episodes recorded before and after the local flowering season in 2006 were analyzed using both models. The results provided an indication of the origins of olive pollen recorded in the city of Córdoba, revealing the influence of three main source areas at specific periods. One area was located nearby, to the southwest of the city (early May), another in the south of the province (mid-May) and the third to the east (late May/early June). The SILAM model yielded more detailed and quantitative results when identifying olive pollen sources and charting transport dynamics. The results from the HYSPLIT trajectory approach and SILAM footprints were qualitatively similar. However, a weak point of back trajectories was their lower sensitivity to details of the transport, as well as the necessity of subjective analysis of the trajectory plots, which were subject for possible misinterpretations. Information on both pollen source locations and local tree flowering phenology was required in order to ensure consistent analysis of the influence of olive sources for both models. Further than this, due to the fact that both models are widely used in other research areas, the results of this work could have a widespread range of application, such as to simulate the transport of radionuclides, e.g., in emergency preparedness exercises.

Keywords Olive pollen dispersion · SILAM · HYSPLIT · Backward trajectories · Source apportionment · Iberian Peninsula

M. A. Hernandez-Ceballos (✉) · J. P. Bolivar
Department of Applied Physics, University of Huelva, Huelva, Spain
e-mail: miguelhceballos@gmail.com

Present Address:
M. A. Hernandez-Ceballos
European Commission, Joint Research Centre, Institute for Transuranium Elements, Ispra, Italy

J. Soares · M. Sofiev
Air Quality Research Department, Finnish Meteorological Institute, Helsinki, Finland

H. García-Mozo · C. Galán
Department of Botany, Ecology and Plant Physiology, Agrifood Campus of International Excellence (CeiA3), University of Córdoba, Córdoba, Spain

1 Introduction

Olive pollen is the most abundant pollen types in southern Europe, due to the large number of olive trees growing and the intense flowering of this anemophilous species. Particularly high counts are recorded in

the southern Spanish region of Andalusia (Fornaciari et al. 2000; Orlandi et al. 2010), the world's leading olive-oil-producing region. The largest olive plantations are concentrated in provinces of Jaén and Córdoba, which together account for 80 % of total Spanish output (Spain produces 33 % of the world's olive oil). Given the major contribution of olive-growing to the local economy, there has been considerable research into various aspects of olive floral phenology, pollen emissions, transport and airborne dispersion; research has also addressed the influence of weather-related factors on airborne pollen counts and their significance for allergy sufferers (Florido et al. 1999; Feo-Brito et al. 2011).

Once pollen is entrained in the atmosphere, the distance that it travels and the final deposition are dependent on atmospheric conditions. Several papers have highlighted the influence of heat-related variables, such as temperature and hours of sunlight on pollen emission, but also pollen transport, gravitational removal and scavenging with precipitation, on temporal and spatial variations in *Olea* pollen counts in Córdoba province (Galán et al. 2005, 2008; García-Mozo et al. 2010).

However, one largely unexplored area of research of olive pollen is the identification of sources contributing to pollen counts and the routes followed by those particles toward the observation points. In this sense, many studies have focused on local release and deposition; however both local and long-distance pollen producers can also play a key role on daily concentrations at a sampling point (Skjoth et al. 2007; Van de Water and Levetin 2001).

Aerobiologists have long sought to obtain detailed knowledge of back trajectories with a view to tracing the transport of airborne pollen (Erdtman 1937). The computation of back trajectory routes helps to identify the origin of airborne biological particles detected at any given sampling point, and to provide detailed data on the long-distance and regional sources of local pollen counts.

It has been used to analyze the peculiarities of airborne birch pollen dispersal in Lithuania (Sauliene and Veriankaite 2006; Veriankaite et al. (2010)), to understand the timing and processes leading to long-distance transport of Agrostis spp. plants in Madras, OR, USA (Van de Water et al. 2007), and to determine the relationship between air mass movements and *Quercus* pollen counts in the Spanish city of Córdoba (Hernández-Ceballos et al. 2011b) and in combination with weather pattern analysis to study the transport (local and long-range components) of *Juniperus ashei* pollen deposition toward the city of Tulsa (Van de Water and Levetin 2001; Van de Water et al. 2003).

The backward trajectory methodology has been also used to study the origin of the observed pollen by Gassmann and Pérez (2006) for *Celtis* and *Nothofagus* pollen in Argentina, by Stach et al. (2007) and Smith et al. (2008) for *Ambrosia* in Poland, by Skjoth et al. (2007) for birch in Poland, by Mahura et al. (2007) and Skjoth et al. (2007, 2008) for birch in Denmark, by Skjøth et al. (2009) for birch in London, etc. The bulk of the works was based on the inverse trajectories computed by the NOAA HYSPLIT model (Draxler et al. 2012), but also by own systems, such as THOR (Skjoth et al. 2002) in Denmark.

With all the simplicity of the approach, the backward trajectory applications usually indicate only the main directions of the transport, ignoring such processes as scavenging with precipitations of the transported pollen clouds, vertical mixing of air masses, etc. As a result, the outcome usually required complicated and subjective analysis of the paths and was not always conclusive. Attempts of quantitative analysis with backward trajectory models are very rare and, to the best of our knowledge, have never been tried for pollen.

A more comprehensive methodology for quantitative analysis of the observational footprints is adjoint dispersion modeling (ADM), which has been applied in several studies at both local and regional scales (Kuparinen 2006; Kuparinen et al. 2007; Saarikoski et al. 2007; Prank et al. 2008) and, in particular, for dispersion of pollen (Sofiev et al. 2006a, b; Siljamo et al. 2008; Veriankaite et al. 2010). ADM, introduced into the atmospheric sciences by Marchuk (1982), is based on the numerical solution of the adjoint dispersion equation. It takes into account atmospheric dispersion and removal processes, and a number of linear (or linearized) chemical and physical transformation processes. ADM provides a quantitative prediction of the geographical location of sources responsible for observed pollen counts and estimates their contribution to those counts. The outcome of the computations also provides an indicator of the sensitivity of observed values to emission fluxes, chemical transformations and the weather events that might affect any given observation.

Both back trajectory and footprint calculations have to be accompanied with knowledge of the geographical distribution and phenological characteristics of pollen sources, as well as with a high temporal resolution pollen concentration data, to clearly identify the origin of measured pollen in a monitoring site (Gassmann and Pérez 2006; Makra et al. 2010).

A number of earlier studies have addressed the spatial and temporal characterization of olive pollen in Córdoba province: Hidalgo et al. (2002) reported on the preliminary phase of an automated system for *Olea* pollen surveying and forecasting, while more recently Hernández-Ceballos et al. (2011a) have analyzed olive pollen transport dynamics throughout the province using back trajectories. Their findings suggest that the high olive pollen counts recorded in the city of Córdoba arise from sources lying to the south and, to a lesser extent, the west of the city. However, their results yielded little specific information regarding the influence of temporal variability on the sources, and source areas were not clearly delimited.

The objectives of the present study were as follows: (1) to identify the source areas contributing to major olive pollen episodes in 2006, by both SILAM and HYSPLIT models, (2) to compare the efficiency of the approaches and (3) to define the temporal influence of each source area on olive pollen counts in the city of Córdoba. This is the first time when the two models have been used in conjunction with a view to enhancing previous data on local *Olea* pollen dynamics.

2 Materials and methods

2.1 Study area

This study was based on the pollen data records (Fig. 1a) for the city of Córdoba, located in southwestern Spain [37°50′N, 4°45′W, 120 m above sea level (m.a.s.l.)]. Local *Olea* pollen counts are among the highest in Spain (Díaz de la Guardia et al. 1999; Garcia-Mozo et al. 2009). The city lies in the center of Córdoba province, an area characterized by marked differences in altitude prompted by differences in relief between the three main geographical areas: the Sierra Morena to the north, the central Guadalquivir valley and the Baetica Mountains to the south. This location gives rise to a Mediterranean climate, typically marked by considerable differences between summer and winter weather conditions. Local weather conditions for 2006–2007 have been outlined by Hernández-Ceballos et al. (2011b), who highlighted the prevalence of surface wind dynamics along the southwest–northeast axis of the Guadalquivir valley.

In order to cover the southern area of the province, where the largest crop sources are to be found, olive counts recorded at Baena (37°37′N; 4°19′W; 363 m.a.s.l)—located 50 km from the city of Córdoba—were also used in this study (Fig. 1b). Floral phenology was surveyed on a weekly basis at 13 points located in different olive-producing areas throughout the province (García-Mozo et al. 2006). Aerobiological and phenological information helped to define the influence of southern areas and to identify pollen transport over the city of Córdoba.

2.2 Pollen observations and phenological data in the city of Córdoba

Bihourly and daily olive pollen counts for 2006 in Córdoba and Baena are analyzed in the present work. Aerobiological data management followed the rules of the Spanish Aerobiology Network (REA) (Galán et al. 2007). Airborne pollen concentrations, both bihourly and daily data, were calculated also following the recommendations of REA, applying in each case the corresponding correction factor which takes into account the sampling time and the analyzed surface under microscope (Galán et al. 2007). Both stations are currently in operation and provide information for the REA (http://www.uco.es/rea). Pollen data were obtained using Hirst-type volumetric spore traps (Hirst 1952) The phenological key developed by Maillard (1975) was used to identify the main stages in floral phenology.

Variations in altitude throughout the province have a direct bearing on the viability of the olive crop owing to the resulting differences in climate. Most olive groves in the south of Córdoba province are located at moderate altitudes, ranging between 200 and 700 m (Fig. 1c). Although most groves are situated 60–80 km from the city of Córdoba, a small number of production areas around 25 km from the city—mostly to the south—were used for phenological observations.

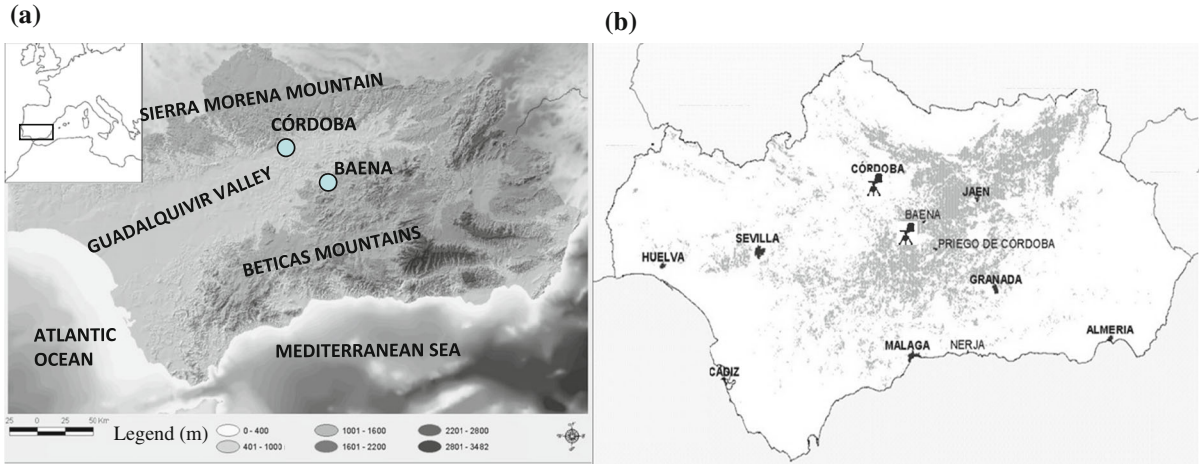

Fig. 1 **a** Orographic characteristics of the study area and **b** location of the main olive pollen crops in Andalusia

2.3 Modeling tools

2.3.1 SILAM dispersion modeling system

One of the modeling tools used in this study was the System for Integrated modeLing of Atmospheric coMposition, SILAM (Sofiev et al. 2006b, 2012b). Its dynamic core currently includes both Eulerian and Lagrangian advection–diffusion formulations. The Eulerian core used in the present study is based on the transport scheme outlined by Galperin (1999, 2000), which incorporates the horizontal diffusion term and is combined with the extended resistance analogy of Sofiev (2002) for vertical diffusion. The system includes a meteorological pre-processor for the evaluation of basic features of the boundary layer and the free troposphere using the meteorological fields provided by numerical meteorological models (Sofiev et al. 2010). Physical–chemical modules of SILAM include several tropospheric chemistry schemes, description of primary anthropogenic and natural aerosols, and radioactive processes. The removal processes are described via dry and wet deposition. Depending on particle size, mechanisms of dry deposition vary from primarily turbulent diffusion-driven removal of fine aerosols to primarily gravitational settling of coarse particles (Slinn and Slinn 1980). Wet deposition distinguishes between sub- and in-cloud scavenging by both rain and snow (Jylha 1991; Sofiev et al. 2006b).

For this study, the model was used for calculating the footprint of the observations at the above sites. The footprint outlines the areas where the sources of the observed concentrations may be located. It can be considered as spatial probability distribution of pollen sources. The pollen observations used as input were compiled from REA observations for the Cordoba and Baena sites. Pollen grains are dispersed as a coarse (about 10 μm in diameter) and chemically inert atmospheric aerosol (Sofiev et al. 2006a).

The timeframe modeled was 54 days, simulating the period from April to June when olive flowering takes place and major pollen episodes are recorded. A time step of 15 min was used, and output was averaged to 1 h. Source apportionment was obtained by evaluating transport over the previous 48 h, for each case of suspected short/medium-range transported pollen recorded at each of the stations. The transport timescale represented the airborne lifetime of pollen species. The Eulerian system was configured to include 8 vertical grid layers up to a height of 6 km above the ground; the lowest level thickness was 20 m. The horizontal grid cell size was 15×15 km^2, and the simulation domain covered the Iberian Peninsula and surrounding area.

The vertical profile of the source term was set as a uniform concentration in the altitude range from 10 to 50 m, while footprint analysis focused on the lowest model layer (0–20 m), where olive trees were located.

2.3.2 Back trajectory HYSPLIT model

Hourly kinematic 3D back trajectories, over a 48-h period and at a final height of 10 m above ground level

(a.g.l), were computed using the Hybrid Single Particle Lagrangian Integrated Trajectory (HYSPLIT) model developed by NOAA's Air Resources Laboratory (ARL) (Draxler et al. 2012). Three-dimensional trajectories were chosen for greater accuracy over other computation methods (e.g., isobaric, isentropic) implemented in the HYSPLIT model. The trajectory is simply the integration of the particle position vector in space and time that is interpolated as the native horizontal coordinate system of meteorological data to an internal terrain-following (σ) vertical coordinate system during computation. The final position is computed from the average velocity at the initial position and the first-guess position.

In both models used in this study, SILAM and HYSPLIT, the weather data were obtained from the European Centre for Medium-Range Weather Forecast (ECMWF, http://www.ecmwf.int) with a 3-h time interval and a spatial resolution of 25x25 km^2 and 75 hybrid vertical levels. This fact ensures to produce a coherent set of results in order to compare these two different approaches.

3 Results

Daily pollen counts in the city of Cordoba during the simulation period from April to June 2006 are shown in Fig. 2a, together with flowering periods for surrounding olive crops (horizontal bar). Some of the main pollen peaks did not coincide with the local flowering period observed in the phenological survey. Minimal pollen counts were recorded prior to the olive flowering stage. Olive pollen was recorded in Córdoba from late April to mid-June, with a significant decline in pollen counts from 19 May onwards. Peak counts were recorded both within and outside the flowering period. Olive pollen counts at the Baena sampling station over 2006 are shown in Fig. 2b; counts were higher than in Córdoba, and flowering took place rather later, in mid-May. Peak counts were recorded only during the flowering period. The post-flowering period in the city of Córdoba broadly coincided with the flowering period in Baena.

Peak pollen days for the city of Córdoba, both inside and outside the full flowering period, were selected and simulated, with a view to identifying and comparing the contributions from different sources to airborne pollen counts in the city of Córdoba, and thus tracing associated pollen transport routes across the province.

The following episodes were analyzed (Fig. 2a): 1 and 6 May (within the flowering period); 13, 19 and 26 May; and 4 and 12 June (outside the flowering period). For each episode, source apportionment was computed using SILAM, and hourly back trajectories were calculated using HYSPLIT, and analyzing bihourly pollen counts at Córdoba and Baena.

3.1 Sources in the southeast

The SILAM predictions for Córdoba and Baena (representing the olive pollen footprint of the previous 48 h), and those of HYSPLIT for Córdoba, for 13 May are shown in Fig. 3, together with bihourly pollen counts at both measurement sites. Pollen counts in the city of Córdoba on 13 May remained around 1,000 pollen grains/m^3 until 18:00 UTC, gradually rising thereafter to peak at 5,000 pollen grains/m^3 at 24:00 UTC; counts in Baena rose from around 2,000 pollen grains/m^3 at 10:00 UTC to a peak of 6,500 pollen grains/m^3 at 18:00 UTC (Fig. 3a), with a large decrease at 12:00 UTC also observed in Cordoba city.

Back trajectories computed by HYSPLIT suggested that the airborne olive pollen recorded during this period at the Córdoba sampling site in all likelihood originated in southern areas (Fig. 3b). The HYSPLIT calculations showed a constant arrival of surface air masses in the course of the day: masses arrived from the south—originating over the Mediterranean Sea and advancing inland up the natural wind channels connecting the Mediterranean coast with the Guadalquivir valley.

The SILAM model prediction for Córdoba (Fig. 3b) indicated the influence of southerly sources located over a wide angle from southwest to southeast of the city. This reflected the southerly location of the province's main olive plantations. Both the HYSPLIT and the olive footprint for the Baena site (Fig. 3b, c) highlighted the considerable influence of sources to the south and the southeast of the site, which were in their flowering period (Fig. 2b), and also of sources further away. Taken in conjunction, these results suggested that the increase in airborne pollen counts in Córdoba city by the end of the day were probably caused by olive pollen transported from southern areas.

In addition, the SILAM model showed other potential sources for the counts recorded in Córdoba,

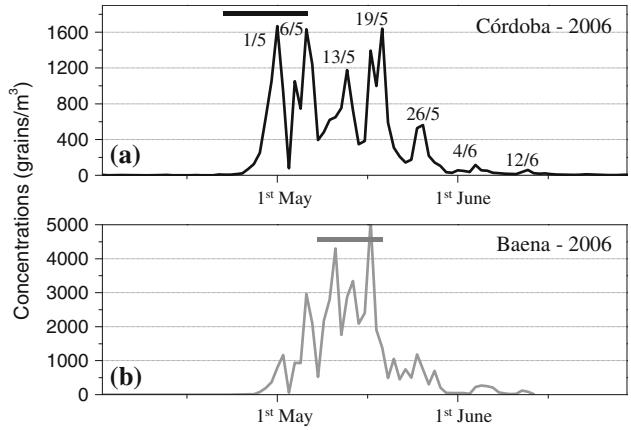

Fig. 2 Daily evolution of *Olea* pollen from April to June in **a** Cordoba and **b** Baena in 2006. *Horizontal bars* represent the time period of full flowering in the olive crop area in the surroundings of Cordoba city and Baena, identified from field phenological observations

located to the southwest of the city, in the Guadalquivir valley (Fig. 3b). HYSPLIT back trajectories did not indicate this influence. Given the distribution of olive crops in the Andalusian region (Fig. 1b) and the similar flowering seasons of olive crops closer to the city, it seems likely that the SILAM footprints provided more accurate and detailed picture than the HYSPLIT trajectories.

The next episode took place a few days later, on 26 May, after the second highest peak was recorded in the city (Fig. 2). Importantly, this peak occurred outside the local flowering periods for both Córdoba and Baena. On that day, the olive pollen count in the city was close to 600 pollen grains/m^3, with two separate trends in the course of the day (Fig. 4a): from 00:00 to 10:00 UTC, counts ranged between 1,000 and 700 pollen grains/m^3; thereafter, counts declined to end close to 400–200 pollen grains/m^3.

The clear difference in counts in the course of the day was not borne out by the HYSPLIT results, which predicted a constant arrival of eastern air masses over Córdoba and Baena that had originated in the Mediterranean Sea (Fig. 4b, c); this would suggest that counts were influenced by olive crops located in the east of the province and beyond (Fig. 1b). This potential contribution was also predicted by the SILAM model over Córdoba, but its importance was lower than the influence of nearby and more southerly sources (Fig. 4b). This was confirmed by the olive footprint for the Baena site (Fig. 4c), but was not picked up by the HYSPLIT trajectories.

Analysis of weather patterns over the city of Córdoba clarified to some extent the characteristics of the episode and accounted for the inconsistency between the SILAM and HYSPLIT simulations. The synoptic conditions on the day were characterized by a high-pressure area which had developed over the Iberian Peninsula. Surface data indicated that under its influence—and as a result of the flow channeling caused by the valley—there was a predominance of northeasterly wind flows over the city during the daytime, veering round to southerly from 18:00 UTC onwards (not shown). These wind dynamics confirmed the combined influence of eastern and southern olive groves revealed by SILAM model predictions.

On 4 June, the SILAM model again predicted a similar influence of eastern and southern areas on airborne pollen counts in the city, which mainly ranged between 100 and 200 pollen grains/m^3, but reached a peak of 250 pollen grains/m^3 at 10:00 UTC (Fig. 5a). On this episode, however, HYSPLIT back trajectories pointed to a constant air mass movement from east, but with a southern influence over Córdoba and Baena, sweeping across the olive groves located in the south of the province (Fig. 5b, c). It therefore seemed plausible that air masses had transported olive pollen from the south but, as in the previous episode, the HYSPLIT model differed from the SILAM model in terms of source area identification over Córdoba city (Fig. 5b), in that trajectories made no clearly reference to eastern sources.

On that day, the surface wind shifted initially from southerly to easterly until 10:00 UTC, when southwesterly/westerly winds became dominant, remaining so thereafter. As a result, both models were able to predict pollen transport from olive groves in the south, as confirmed by the SILAM result in Baena (Fig. 5c)

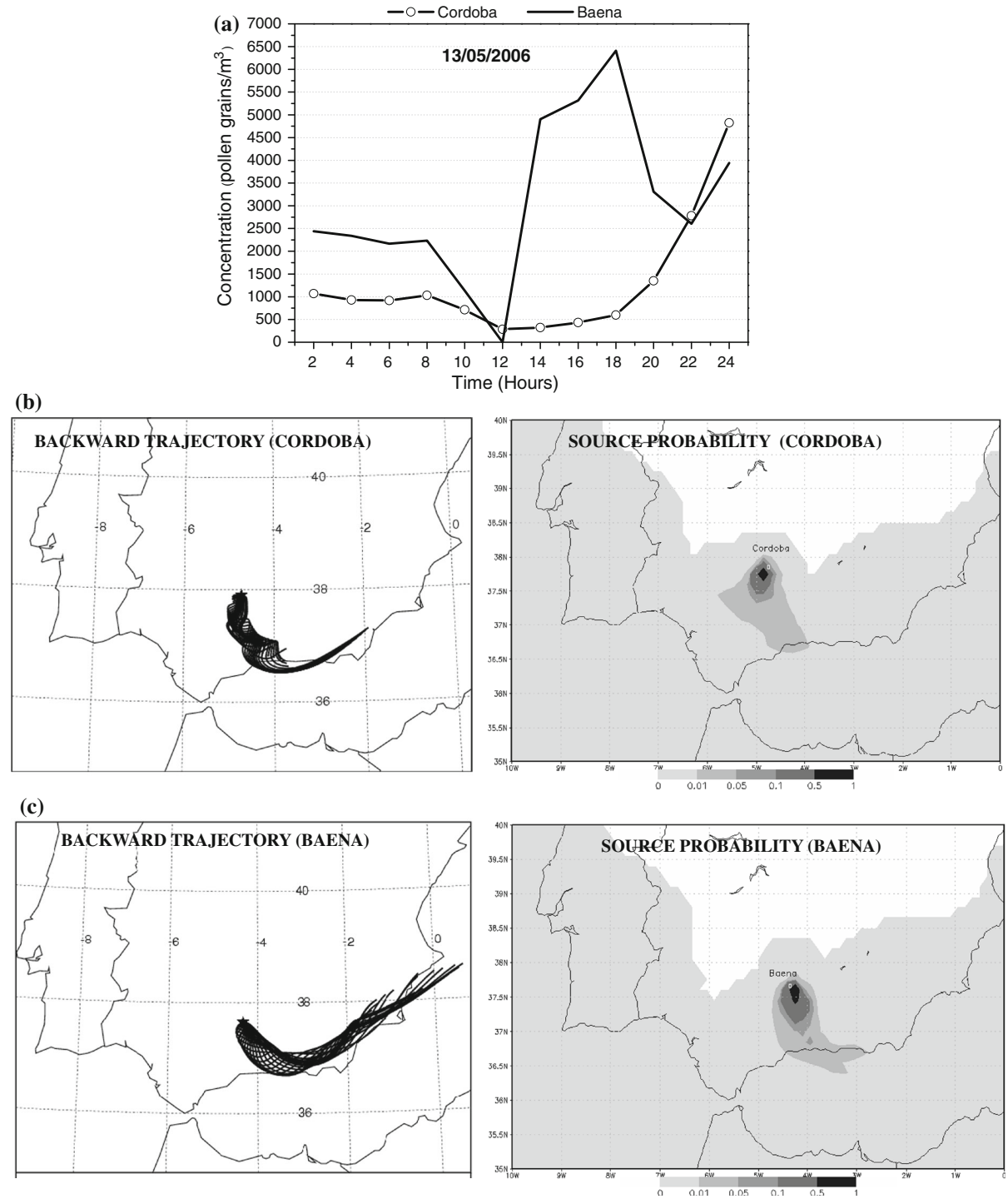

Fig. 3 **a** Bihourly olive pollen concentrations at Cordoba and Baena sites for May 13, 2006, **b** hourly 48-h HYSPLIT backward trajectories at 10 m and the predicted 48-h footprint using Eulerian SILAM model for **b** Cordoba city and **c** Baena site

and bihourly data from the Córdoba and Baena sampling sites, but HYSPLIT suggests no influence of eastern sources.

The two models displayed similar behavior on 12 June (not shown), with a marked similarity in results between both sampling sites until 22:00 UTC, when a

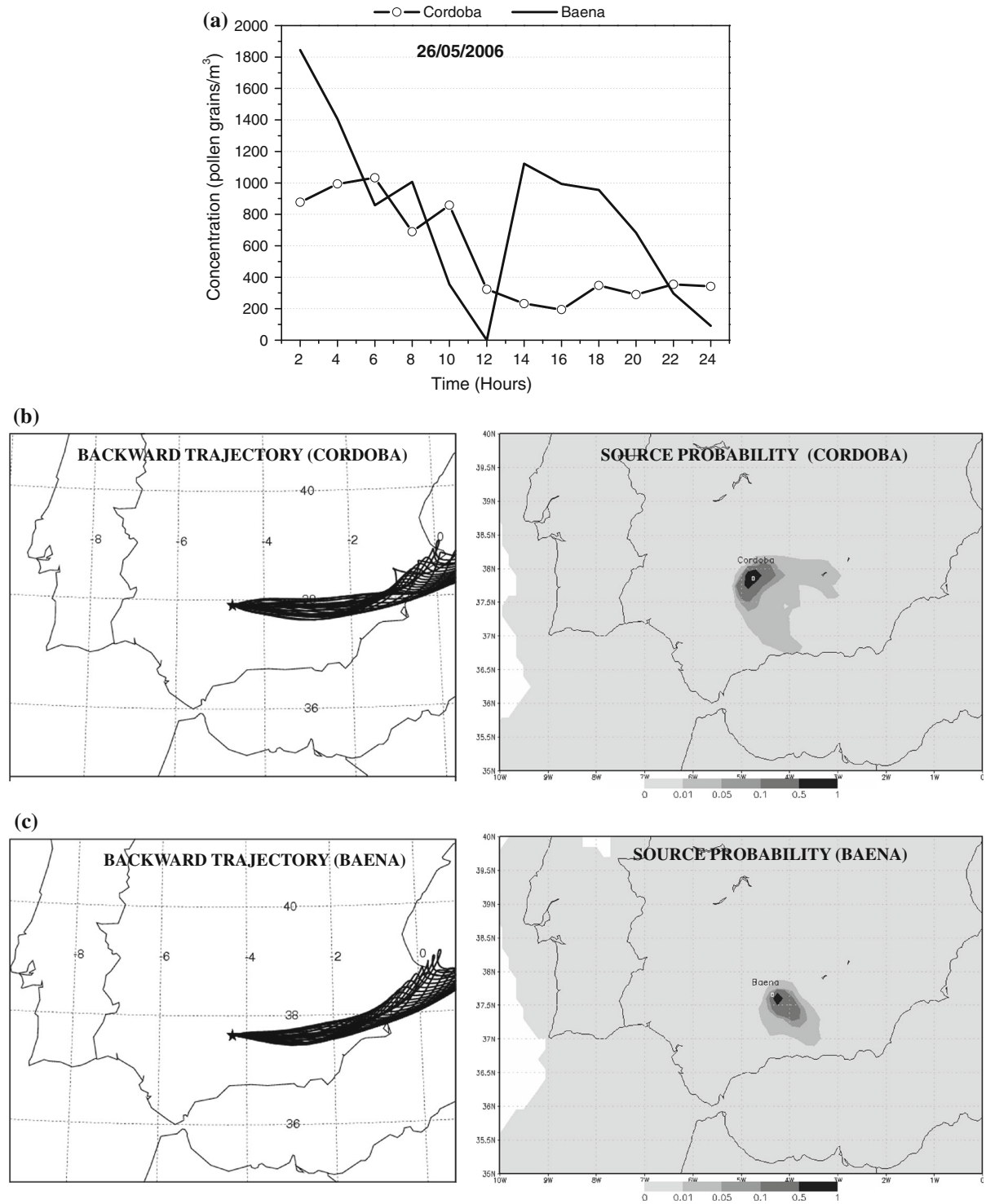

Fig. 4 **a** Bihourly olive pollen concentrations at Cordoba and Baena sites for May 26, 2006, hourly 48-h HYSPLIT backward trajectories at 10 m and the predicted 48-h footprint using Eulerian SILAM model for **b** Cordoba city and **c** Baena site

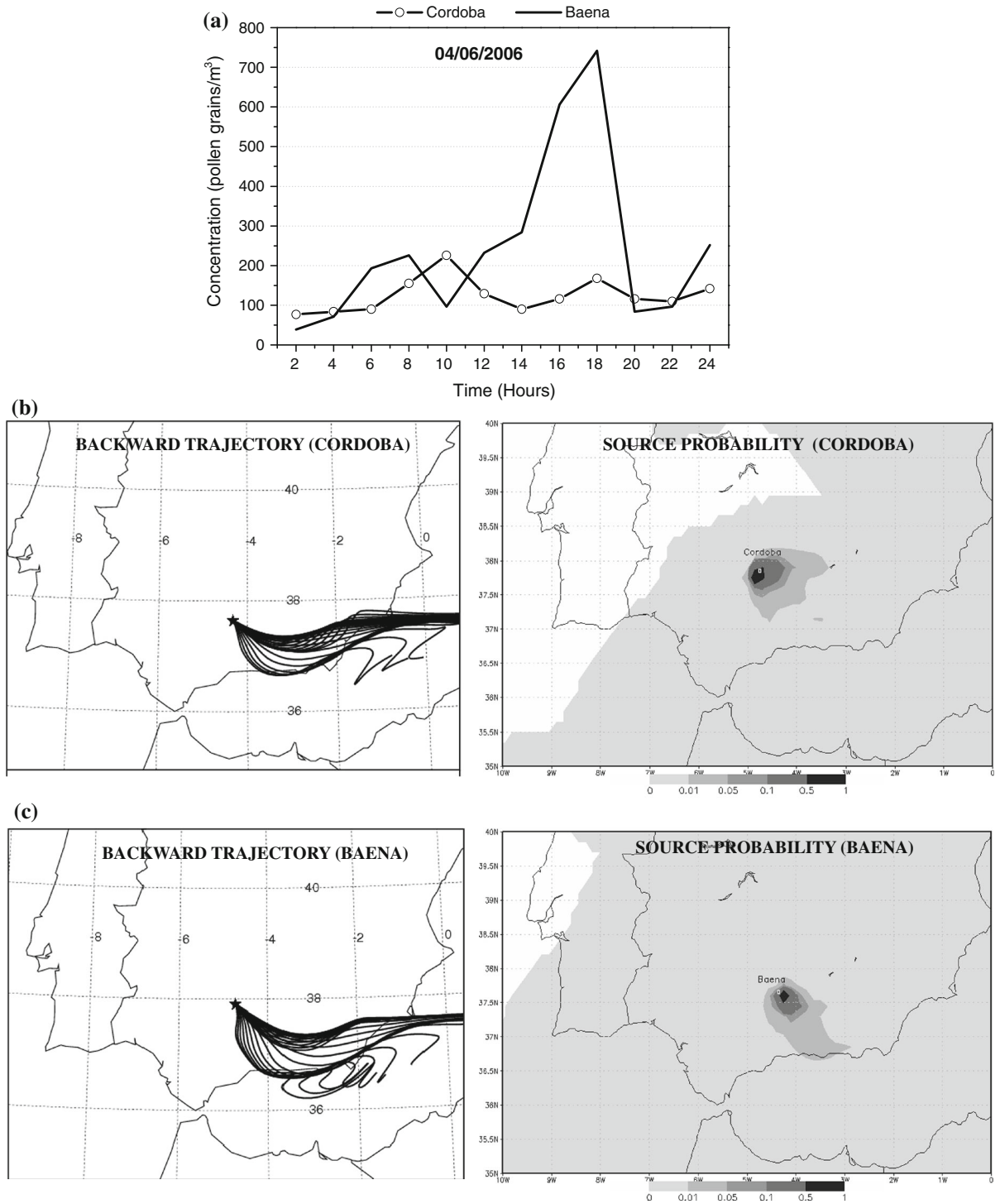

Fig. 5 **a** Bihourly olive pollen concentrations at Cordoba and Baena sites for 4th June 2006, hourly 48-h HYSPLIT backward trajectories at 10 m and the predicted 48-h footprint using Eulerian SILAM model for **b** Cordoba city and **c** Baena site

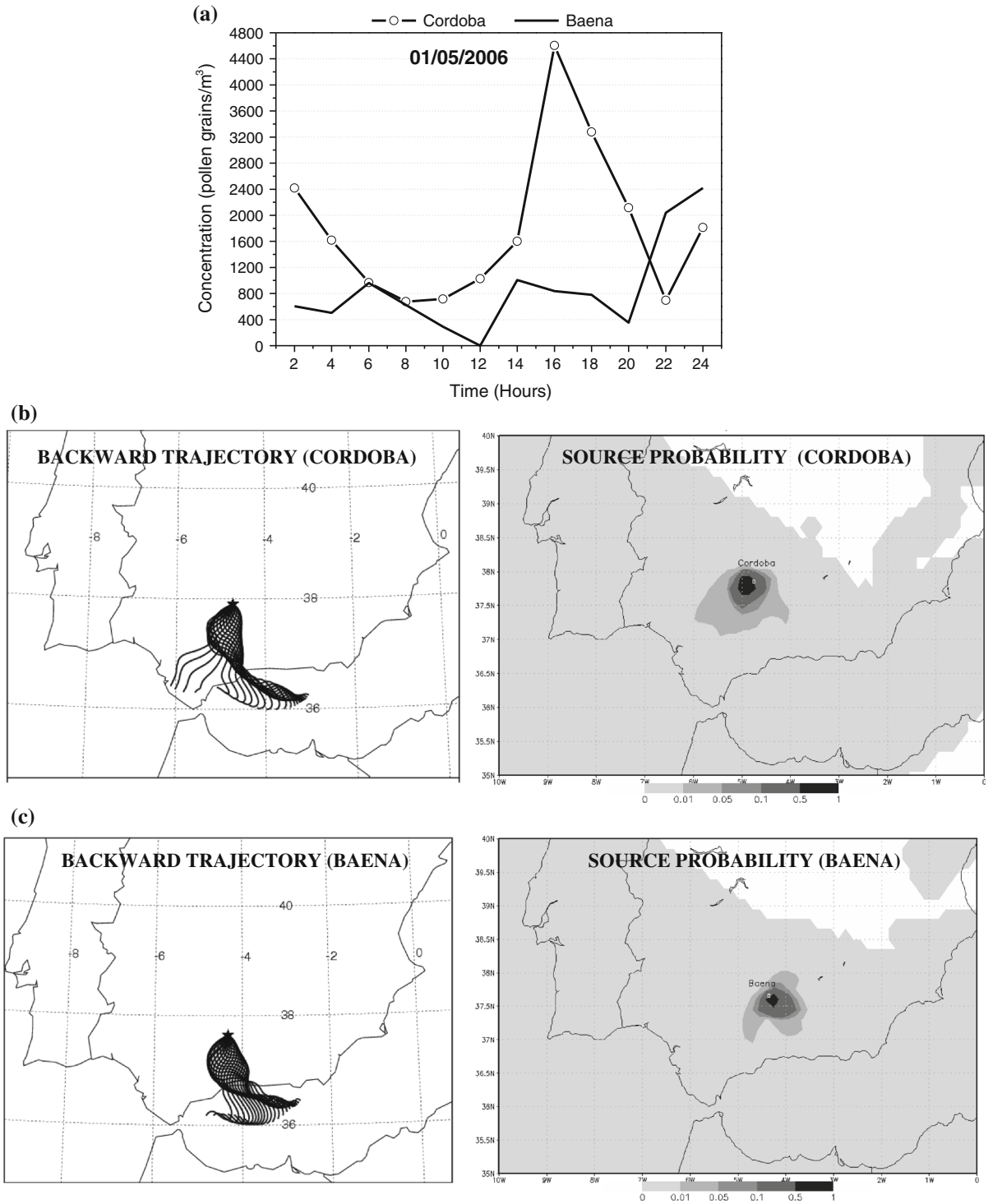

Fig. 6 **a** Bihourly olive pollen concentrations at Cordoba and Baena sites for May 1, 2006, hourly 48-h HYSPLIT backward trajectories at 10 m and the predicted 48-h footprint using Eulerian SILAM model for **b** Cordoba city and **c** Baena site

sudden sharp increase in pollen counts was recorded at Baena. In this episode, as earlier, the SILAM model clearly showed that the Baena area was outside the strong probability zone for high pollen counts due to eastern sources.

3.2 Sources in the southwest

Findings for the May 1 episode showed disparate trends in olive pollen counts in Córdoba and Baena until the afternoon (Fig. 6a). Córdoba displayed two peaks, one at 02:00 UT (2,400 pollen grains/m^3) and the most intense at 16:00 UTC (4,400 pollen grains/m^3), while counts at Baena rose from 20:00 UTC onwards, reaching values of 2,400 pollen grains/m^3; no earlier peaks were recorded, values remaining below 1,000 pollen grains/m^3. Given that this episode day coincided with the full flowering of olives on the outskirts of the city (Fig. 2c), the sharp increase in airborne pollen counts in Córdoba might be attributable to local sources located close to the river in lowland arable areas.

The set of back trajectories computed by HYSPLIT (Fig. 6b, c) showed a scarce variation in surface air mass movements in the course of the day, keeping in a southerly movement during the day; however, in the early hours, the air masses swept across the olive groves in the south and, then, progressively channeled toward the city by the Guadalquivir valley.

The SILAM simulation indicated a greater contribution from local pollen sources to pollen counts in the city of Córdoba (Fig. 6b). Other potential contributors included areas to the southwest of the city, coinciding with the air mass movements predicted by back trajectories. The SILAM model also clearly showed that the Baena area was outside the strong probability zone for high pollen counts (Fig. 6c).

The SILAM results indicated pollen transport from Córdoba to Baena, showing that pollen counts in Baena were influenced by northern sources, i.e., located to the south of Córdoba city, in the surrounding countryside.

Similar results were obtained for the 6 May episode. SILAM model highlighted the influence of pollen sources on the outskirts of the city and on the southwest, from olive groves in the Guadalquivir valley (Fig. 7b), on pollen counts in the city of Córdoba, which generally ranged around 1,000 pollen grains/m^3 but peaked at 14:00 UTC (5,000 pollen grains/m^3) (Fig. 7a). In this case, HYSPLIT trajectory model indicated this influenced with trajectories originated to the north of the province, which presented a progressive clockwise movement during the day, with final arrival from the south/southwest over Cordoba and Baena (Fig. 7b, c).

SILAM predictions again indicated the probable influence of northern sources on Baena pollen counts (Fig. 7c). A peak was recorded at Baena (7,000 pollen grains/m^3) at the same time as in Córdoba (14:00 UTC), followed by a further sharp peak (20,000 pollen grains/m^3 at 18:00 UTC), probably attributable to short-range transport.

The last episode took place on 17 May, when olive pollen counts peaked at 1,636 grains/m^3 in the city of Córdoba, then gradually declined from 02:00 UTC (3,250 pollen grains/m^3) until 08:00 UTC (1,500 pollen grains/m^3), thereafter remaining at around that level for the rest of the day (Fig. 8a).

The computation of back trajectories over the city of Córdoba and Baena revealed a constant westerly flow throughout the day, originating over the Atlantic Ocean (Figs. 8b,c); this suggested that pollen counts might be associated with olive groves in the west/northwest. This was supported by SILAM predictions (Fig. 8b), which did not predict the arrival of olive pollen in the city from southern olive groves. In subsequent episodes, SILAM results indicated probable transport of pollen from northern sources to the south of the province (Fig. 8c), which appears to be borne out by the peak observed in Baena coinciding with a drop in pollen counts in the city of Córdoba.

4 Discussion

The most striking finding reported by Hernández-Ceballos et al. (2011a) was the existence of two major types of moving air masses associated with high olive pollen counts in the city of Córdoba: one from the south/southeast and the other from the west. These results were obtained computing back trajectories at a final height of 500 m by the use of GDAS (Global Data Assimilation System) meteorological files with a spatial resolution of 111 km. In this study, the use of ECMWF meteorological files, with horizontal spatial resolutions of 25 km, over four times denser than GDAS, has allowed to determine with more detail the dynamic (transport, advection and dispersion) of olive pollen in southern Iberian Peninsula.

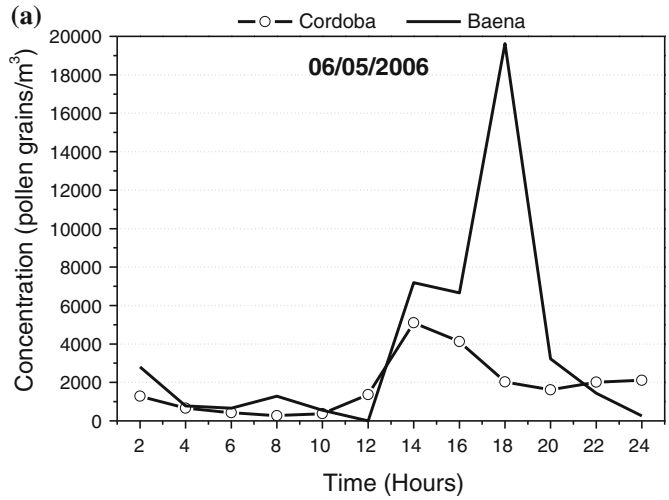

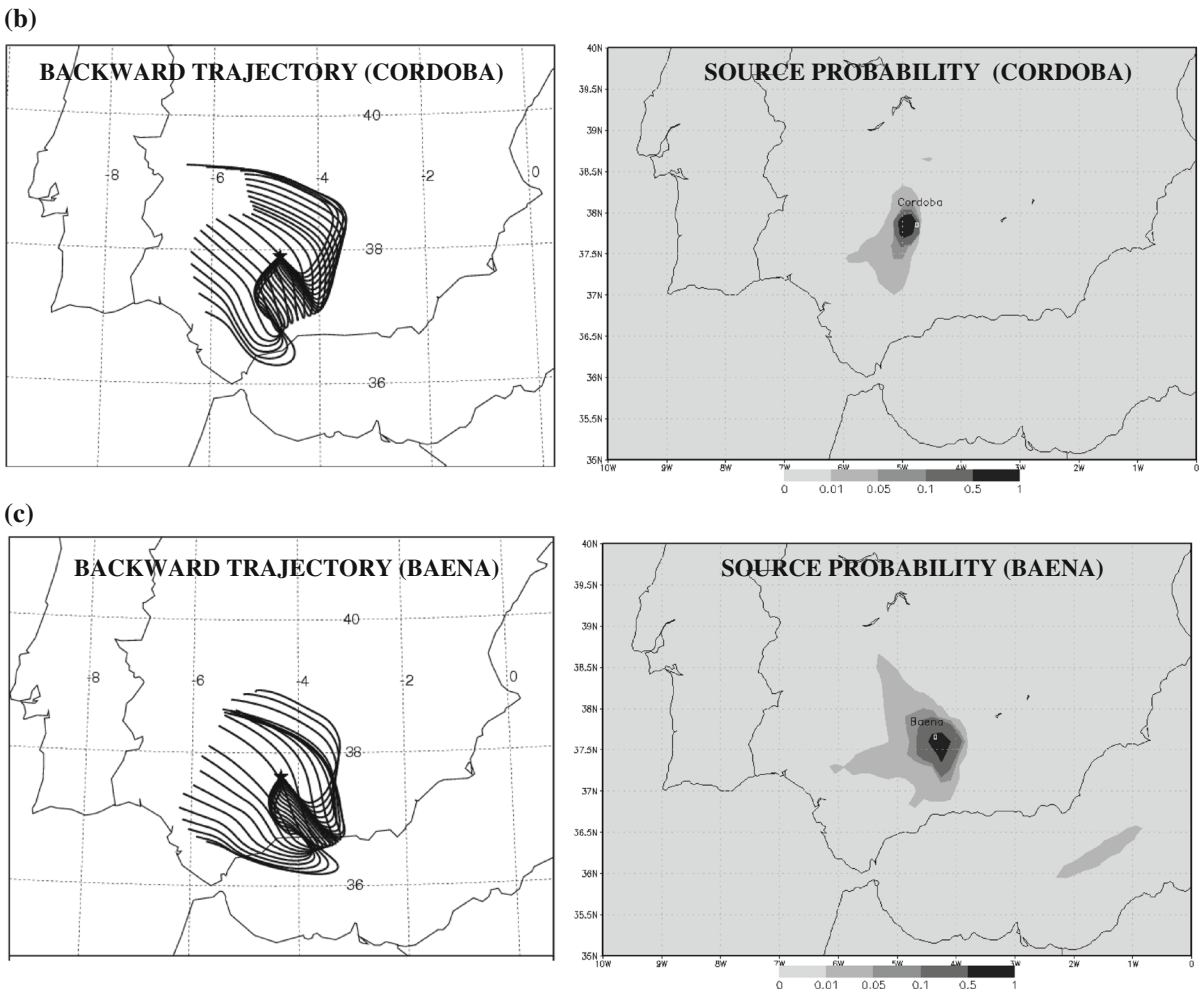

Fig. 7 **a** Bihourly olive pollen concentrations at Cordoba and Baena sites for May 6, 2006, hourly 48-h HYSPLIT backward trajectories at 10 m and the predicted 48-h footprint using Eulerian SILAM model for **b** Cordoba city and **c** Baena site

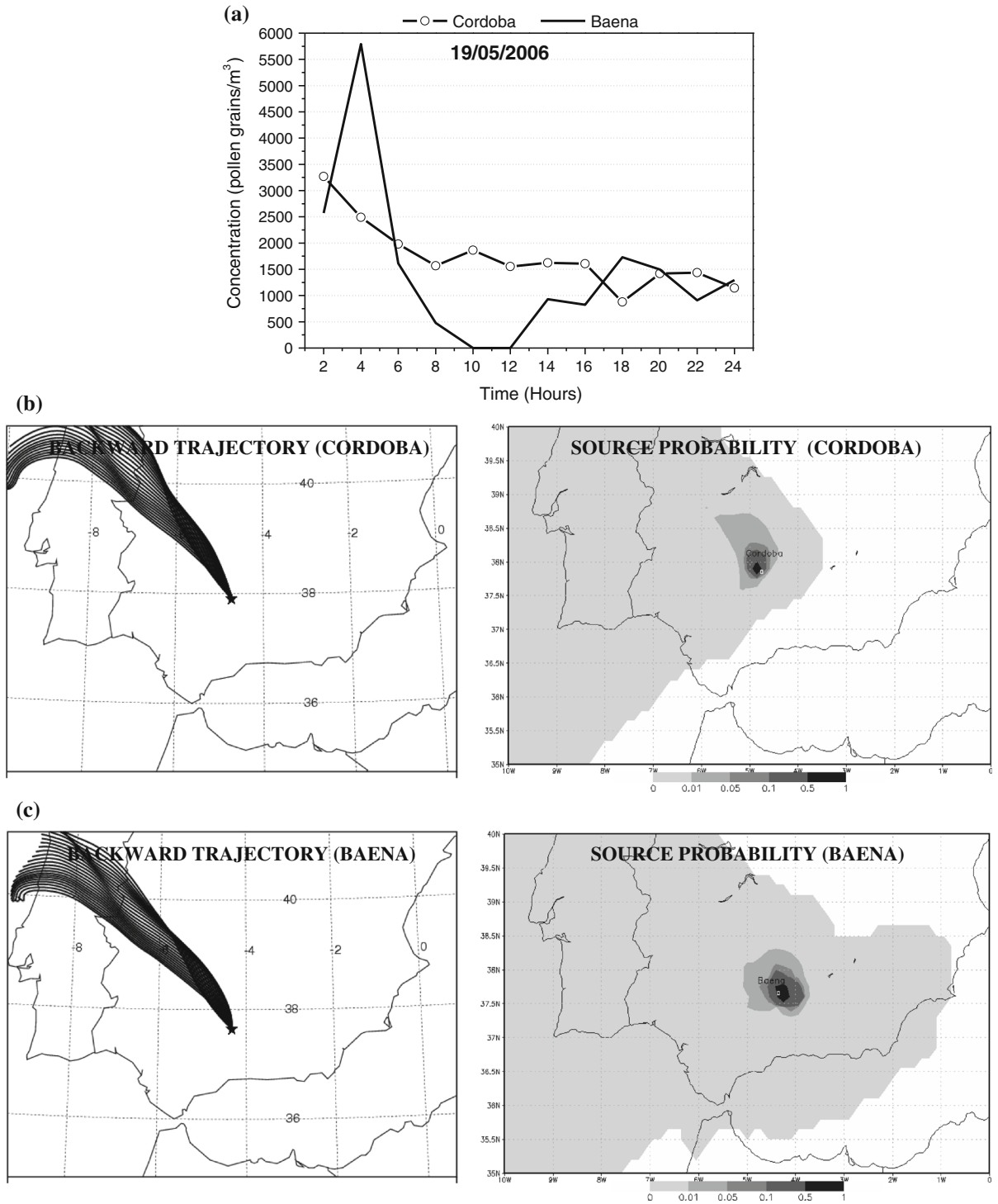

Fig. 8 **a** Bihourly olive pollen concentrations at Cordoba and Baena sites for May 19, 2006, hourly 48-h HYSPLIT backward trajectories at 10 m and the predicted 48-h footprint using Eulerian SILAM model for **b** Cordoba city and **c** Baena site

As reported by Veriankaite et al. (2010), approaches based on the data from only a few trajectories may encounter difficulties, particularly in cases with complex atmospheric patterns. Here, periods were mainly governed by a synoptic configuration, characterized by a weak pressure gradient. This usually gives rise to local or mesoscale winds, which tend to be characterized by low wind speeds and rapid changes in wind direction, and are determined by local temperatures and land relief. Furthermore, Pérez-Landa et al. (2007a, b) have noted how difficult and complex it is to quantify airflow patterns over mountains, given the anabatic and katabatic flows characteristic of this type of atmospheric transport model. Under these circumstances, the use of higher spatial resolution to compute trajectories with HYSPLIT as well as to determine the pollen dispersion with SILAM model has allowed to consider with more detail the surface winds and, therefore, has increased the quality and the validity of the results concerning the olive pollen transport.

Considering these meteorological factors and the differences in the determination of source influences, as indicated under Materials and Methods, the HYSPLIT trajectory and SILAM models have achieved an acceptable approximation in their predictions. In this sense, the results also highlighted the similarity of episode simulations heavily influenced by olive groves close to the city of Córdoba, as shown on 1, 6 and 19 May.

Results allowed for linking the pollen counts in Córdoba to three major emission sources, located both within and beyond the province of Córdoba. The first source area to be identified was located in the outskirts of the city itself, to the west/southwest of the sampling site, along the Guadalquivir valley. This area was well defined by the SILAM model, confirming the hypothesis put forward by Hernández-Ceballos et al. (2011a) regarding the influence of western sources. That influence was apparent in the episodes of May 1, 6 and 19, which also pointed to the transport of pollen from northern olive groves to southern areas of the province.

The second source was identified as an area of extensive olive groves in the south of the province, confirming the south–north gradient reported for *Olea* pollen sources. The identification of the south as a source of airborne pollen in the city of Córdoba is borne out by the findings of Hidalgo et al. (2002) and Hernández-Ceballos et al. (2011a) regarding the considerable influence of pollen released in this area, illustrated here in the episodes of 13 and 26 May.

These simulations also enabled the identification of another pollen source located to the east of the city. This area contains Andalusia's most extensive olive groves, in the province of Jaén. Although its influence has not been scientifically demonstrated in earlier modeling studies, research into olive aerobiology and phenology in this area shows that recorded phenological and pollen data support the idea of this being a likely transport route (Aguilera and Ruiz Valenzuela 2011). During the present research, several examples of pollen input from eastern sources were found in the city of Córdoba, for example, in the 26 May and 4 June episodes.

The results of the present study also highlighted the influence of sources located to the north of the city of Córdoba. This olive production area, in direct contrast to western local sources, displays distinct phenological behavior influenced by differences in weather patterns, mainly involving temperature and relative humidity (Orlandi et al. 2005).

Variations in the timing of pollen emission were defined by analyzing the dates on which each olive pollen source was present in the city of Córdoba. This variability clearly reflected differences in the flowering period of olive-producing areas throughout the province. The flowering of olive trees in the immediate vicinity of the city of Córdoba in early May led to pollen counts attributable to nearby sources and southwestern source at that time. By mid-May, coinciding with the flowering period for crops in the south of the province, olive pollen counts in Córdoba were mainly attributable to sources to the south of the city. These results confirmed earlier estimates based on the contribution of southern olive groves to the pollen curve recorded in the city, once the flowering period of nearby sources was over (Fornaciari et al. 2000). After the main flowering season, in late May and early June, pollen peaks confirmed the increasing predominance of eastern sources. These findings enabled a preliminary identification of the real origins of airborne pollen in the city of Córdoba. These results, in the spatial scale of Cordoba province, are in agreement with studies that indicate that daily pollen concentrations can be affected by different pollen producers and so, by several types of pollen transport (local, regional or long-distance) (Van de Water and Levetin 2001; Skjoth et al. 2007).

Results have also indicated the existence of differences between SILAM and HYSPLIT predictions. In some episodes, the SILAM model simulated a branching of the footprint due to a rapid change in wind direction, which was not observed by HYSPLIT trajectories. The most evident explanation for this effect is underrepresentation of variability of atmospheric transport if a few trajectories are used to describe it. In most cases, they would simply follow the most probable path missing other branches and underrepresenting the width of the plumes. This problem is somewhat reduced in Lagrangian particle models but is still significant even there (Veriankaite et al. 2010, Sofiev et al. 2012a). Apart from a possibility to consider species transformations and removal, a possibility to represent the full range of the variability of the atmospheric transport is probably the main advantage of the Eulerian paradigm for ADM.

This fact has been observed in the combined influence of southern and eastern sources. For instance, this influenced was observed by SILAM model on 13 and 26 May, and 4 June, but was not defined by back trajectories, which present a time-stable transport direction during these days and so, suggesting only one source apportionment. In this case, these differences are not associated with the use of different weather file and are related to the characteristics used to compute backward trajectories (HYSPLIT) and the adjoint simulation (SILAM), previously commented in Sect. 2.3.

These differences between models also confirmed the need for accurate information concerning the location of sources and their flowering periods, particularly when computing back trajectories, since this tool indicates only the horizontal and vertical movement of air masses over a previous period. In that sense, SILAM generally proved to be more versatile when evaluating pollen sources. Similar findings are reported by Veriankaite et al. (2010), who conclude that adjoint computations provide a more comprehensive and less subjective approach to the identification of pollen emission sources.

Accurate analysis of biological particle dynamics requires rigorous prior examination of the characteristics of each modeling tool used, together with a clear understanding of the purposes of the study. According to the above-presented results, the footprint analysis seems to be more accurate than the back trajectory calculations for the episodes considered in the present study.

5 Conclusions

The present study compared the results obtained for airborne olive pollen dispersion in the province of Córdoba obtained using two different methods: computation of back trajectories using the HYSPLIT model and the SILAM model. Using data for 2006, a set of daily episodes were studied in which high pollen counts were recorded in the city of Córdoba—both within and outside the flowering period of nearby olive crops—in order to determine the apportionment of olive pollen sources.

The predictions of the SILAM model indicated three main source areas for airborne olive pollen in the city of Córdoba; the influence of each was determined by variations in timing. Pollen from the first source, located in the south of the province, predominated in early May; the second source, dominant in mid-May, was located both in the immediately surroundings of the city of Córdoba and in an area to the southwest of the monitoring site, along the Guadalquivir valley; the third source was situated to the east of the city and predominated in late May and early June.

The HYSPLIT trajectory analysis proved less accurate for defining olive pollen dynamics in southern Spain. To better understand HYSPLIT results, precise information on the location of pollen sources and on flowering phenology is essential. Comparison of the performance of the two modeling tools for apportioning pollen sources showed that SILAM was the more versatile of the two.

Acknowledgments The authors are grateful to the European Social Fund and the Spanish Science Ministry for joint financing. Dr. García Mozo was supported by a "Ramón y Cajal" contract, and the Andalusia Regional Government funded the project entitled "Analisis de la Dinamica del Polen Atmosferico en Andalucia" (RNM-5958). The authors also thank the Science and Innovation Ministry for funding the project entitled "Impacto del Cambio Climatico en la Fenologia de especies vegetales del Centro y Sur de la Peninsula Iberica" (FENOCLIM) CGL2011-24146. Support from the EU FP7-HIALINE project is gratefully acknowledged. The authors gratefully acknowledge the NOAA Air Resources Laboratory (ARL) for the provision of the HYSPLIT transport model and READY Web site (http://ready.arl.noaa.gov) used in this publication.

References

Aguilera, F., & Ruiz Valenzuela, L. (2011). Altitudinal fluctuation in the pollen olive emission: an approximation from the olive groves of the south-east Iberian Peninsula. *Aerobiologia*. doi:10.1007/s10453-011-9244-9.

Díaz de la Guardia, C., Galán, C., Domínguez, E., Alba, F., Ruiz, L., Sabariego, S., et al. (1999). Variations in the main pollen season of *Olea europaea* L. at selected sites in the Iberian Peninsula. *Polen, 10*, 103–113.

Draxler, R. R., Stunder, B., Rolph, G., Stein, A., & Taylor, A. (2012). HYSPLIT_4. User's Guide, via NOAA ARL. http://www.arl.noaa.gov/documents/reports/HYSPLIT_user_guide.pdf. NOAA Air Resources Laboratory, Silver Spring, MD, Dec., 1997 revised March, 2012.

Erdtman, G. (1937). Pollen grains recovered from the atmosphere over the Atlantic. *Acta Horticulturae Gothoburg, 12*, 185–196.

Feo-Brito, F., Mur-Gimeno, P., Carnés, J., Martín, R., Fernández-Caldas, E., Lara, P., et al. (2011). *Olea europea* pollen counts and aeroallergen levels predict clinical symptoms in patients allergic to olive pollen. *Annals of Allergy, Asthma & Immunology, 106*, 146–152.

Florido, J. F., González Delgado, P., Saenz de San Pedro, B., Quiralte, J., Arias de Saavedra, J. M., Peralta, V., et al. (1999). High levels of *Olea europaea* pollen and relation with clinical findings. *Annals of Allergy, Asthma & Immunology, 119*, 133–137.

Fornaciari, M., Galán, C., Mediavilla, A., Domínguez, E., & Romano, B. (2000). Aeropalynological and phenological study in two different olive Mediterranean areas: Córdoba (Spain) and Perugia (Italia). *Plant Biosystems, 134*, 199–204.

Galán, C., Cariñanos, P., Alcázar, P., & Domínguez, E. (2007). Management and quality manual. Spanish aerobiology network (REA). Córdoba, Spain: Servicio Publicaciones Universidad de Córdoba. ISBN 978-84-690-6353-8.

Galán, C., García-Mozo, H., Vázquez, L., Ruiz, L., Díaz de la Guardia, C., & Domínguez, E. (2008). Modelling olive (*Olea europaea* L.) crop yield in Andalusia Region, Spain. *Agronomy Journal, 100*, 98–104.

Galán, C., García-Mozo, H., Vázquez, L., Ruiz, L., Díaz de la Guardia, C., & Trigo, M. M. (2005). Heat requirement for the onset of the *Olea europaea* L. pollen season in several sites in Andalusia and the effect of the expected future climate change. *International Journal of Biometeorology, 49*, 184–188.

Galperin, M. V. (1999). Approaches for improving the numerical solution of the advection equation. In Z. Zlatev, J. Dongarra, I. Dimov, J. Brandt, & P. J. Builtjes (Eds.), *Large scale computations in air pollution modelling* (pp. 161–172). The Netherlands: Kluwer Academic Publishers.

Galperin, M. V. (2000). The approaches to correct computation of airborne pollution advection. In: Problems of ecological monitoring and ecosystem modelling (vol. XVII, pp. 54–68). St. Petersburg: Gidrometeoizdat (in Russian).

García-Mozo, H., Galán, C., & Vazquez, L. (2006). The reliability of geostatistic interpolation in olive field phenology. *Aerobiologia, 22*, 97–108.

García-Mozo, H., Mestre, A., & Galán, C. (2010). Phenological trends in southern Spain: A response to climate change. *Agricultural and Forest Meteorology, 150*, 575–580.

Garcia-Mozo, H., Orlando, F., Galan, C., Fornaciari, M., Romano, B., Ruiz, L., et al. (2009). Olive flowering phenology variation between different cultivars in Spain and Italy: Modelling analysis. *Theoretical and Applied Climatology, 95*, 385–395.

Gassmann, I. M., & Pérez, F. C. (2006). Trajectories associated to regional and extra-regional pollen transport in the southeast of Buenos Aires province, Mar del Plata (Argentina). *International Journal of Biometeorology, 50*, 280–291.

Hernández-Ceballos, M. A., García-Mozo, H., Adame, J. A., Domínguez-Vilches, E., Bolívar, J. P., De la Morena, B. A., et al. (2011a). Determination of potential sources of *Quercus* airborne pollen in Córdoba city (southern Spain) using back-trajectory analysis. *Aerobiologia, 27*, 261–276.

Hernández-Ceballos, M. A., García-Mozo, H., Adame, J. A., Domínguez-Vilches, E., De la Morena, B. A., Bolívar, J. P., et al. (2011b). Synoptic and meteorological characterization of olive pollen transport in Cordoba province (Southwestern Spain). *International Journal of Biometeorology, 55*, 17–34.

Hidalgo, P. J., Mangin, A., Galán, C., Hembise, O., Vázquez, L. M., & Sanchez, O. (2002). An automated system for surveying and forecasting *Olea* pollen dispersion. *Aerobiologia, 18*, 23–31.

Hirst, J. (1952). An automatic volumetric spore-trap. *Annals of Applied Biology, 36*, 257–265.

Jylha, K. (1991). Empirical scavenging coefficients of radioactive substances released from Cernobyl. *Atmospheric Environment, 25A*, 263–270.

Kuparinen, A. (2006). Mechanistic models for wind dispersal. *Trends in Plant Science, 11*, 298–301.

Kuparinen, A., Markkanen, T., Riikonen, H., & Vesala, T. (2007). Modelling air-mediated dispersal of spores, pollen and seeds in forested areas. *Ecological Modelling, 208*, 177–188.

Mahura, A., Korsholm, S. U., Baklanov, A. A., & Rasmussen, A. (2007). Elevated birch pollen episodes in Denmark: contributions from remote sources. *Aerobiologia, 23*, 171–179.

Maillard, R. (1975). *L'olivier*. Paris, France: INVUFLEC.

Makra, L., Sánta, T., Matyasovszky, I., Damialis, A., Karatzas, K., Bergmann, K.-C., et al. (2010). Airborne pollen in three European cities: Detection of atmospheric circulation pathways by applying three-dimensional clustering of backward trajectories. *Journal of Geophysical Research, 115*, D24220.

Marchuk, G. I. (1982). *Mathematical modeling in the environmental problems* (p. 320). Moscow: ''Nauka'' Publisher. (in Russian).

Orlandi, F., Garcia-Mozo, H., Galán, C., Romano, B., Diaz de la Guardia, C., Ruiz, L., et al. (2010). Olive flowering trends in a large Mediterranean area (Italy and Spain). *International Journal of Biometeorology, 54*, 151–163.

Orlandi, F., Vazquez, L. M., Ruga, L., Bonofiglio, T., Fornaciari, M., García-Mozo, H., et al. (2005). Bioclimatic requirements for olive flowering in two Mediterranean Regions located at the same latitude (Andalucía, Spain, and

Sicily, Italy). *Annals of Agricultural and Environmental Medicine, 12*, 47–52.

Pérez-Landa, G., Ciais, P., Gangoiti, G., Palau, J. L., Carrara, A., Gioli, B., et al. (2007a). Mesoscale circulations over complex terrain in the Valencia coastal region, Spain—Part 2: Modeling CO2 transport using idealized surface fluxes. *Atmospheric Chemistry and Physics, 7*, 851–1868.

Pérez-Landa, G., Ciais, P., Sanz, M. J., Gioli, B., Miglietta, F., Palau, J. L., et al. (2007b). Mesoscale circulations over complex terrain in the Valencia coastal region, Spain–Part 1: Simulation of diurnal circulation regimes. *Atmospheric Chemistry and Physics, 7*, 1851–1868.

Prank, P., Sofiev, M., Kaasik, M., Ruuskanen, T., Kukkonen, J., & Kulmala, M. (2008). The origin and formation mechanics of aerosol during a measurement campaign in Finnish Lapland, evaluated using the regional dispersion model SILAM. In C. Borrego & A. I. Miranda (Eds.), *Air pollution modeling and its application XIX, NATO science for peace and security series-C: Environmental security* (pp. 530–538). Berlin: Springer.

Saarikoski, S., Sillanpää, M., Sofiev, M., Timonen, H., Saarnio, K., Teinilä, K., et al. (2007). Chemical composition of aerosols during a major biomass burning episode over northern Europe in spring 2006: Experimental and modelling assessments. *Atmospheric Environment, 41*, 3577–3589.

Sauliene, I., & Veriankaite, L. (2006). Application of backward air mass trajectory analysis in evaluating airborne pollen dispersion. *Journal of Environmental Engineering and Landscape Management, 14*, 113–120.

Siljamo, P., Sofiev, M., Severova, E., Ranta, H., Kukkonen, J., & Polevova, S. (2008). Sources, impact and exchange of early-spring birch pollen in the Moscow region and Finland. *Aerobiologia.* doi:10.1007/s10453-008-9100-8.

Skjoth, C. A., Hertel, O., & Ellermann, T. (2002). Use of the ACDEP trajectory model in the Danish nation-wide Background Monitoring Programme. *Physics and Chemistry of the Earth, 27*, 1469–1477.

Skjøth, C. A., Smith, M., Brandt, J., & Emberlin, J. (2009). Are the birch trees in Southern England a source of pollen in North London? *International Journal of Biometeorology, 53*, 75–86.

Skjoth, C. A., Sommer, J., Brandt, J., Hvidberg, M., Geels, C., Hansen, K. M., et al. (2008). Copenhagen—a significant source to birch (*Betula*) pollen? *International Journal of Biometeorology, 52*, 453–462.

Skjoth, C. A., Sommer, J., Stach, A., Smith, M., & Brandt, J. (2007). The long-range transport of birch (*Betula*) pollen from Poland and Germany causes significant pre-season concentrations in Denmark. *Clinical and Experimental Allergy, 37*, 1204–1212.

Slinn, S. A., & Slinn, W. G. N. (1980). Predictions for particle deposition on natural waters. *Atmospheric Environment Part A General Topics, 14*, 1013–1016.

Smith, M., Skjøth, C. A., Myszkowska, D., Uruska, A., Puc, M., Stach, A., et al. (2008). Long-range transport of Ambrosia pollen to Poland. *Agricultural and Forest Meteorology, 14*, 1402–1411.

Sofiev, M. (2002). Extended resistance analogy for construction of the vertical diffusion scheme for dispersion models. *Journal of Geophysical Research Atmosphere, 107*, ACH 10-1–ACH 10-8.

Sofiev, M., Belmonte, J., Gehrig, R., Izquierdo, R., Smith, M., Dahl, A., et al. (2012a). Chapter 5. Airborne pollen transport. In M. Sofiev & K.-C. Bergman (Eds.), *Allergenic pollen. A review of the production, release, distribution and health impacts* (pp. 127–161). Dordrecht: Springer.

Sofiev, M., Genikhovich, E., Keronen, P., & Vesala, T. (2010). Diagnosing the surface layer parameters for dispersion models within the meteorological-to-dispersion modeling interface. *Journal of Applied Meteorology and Climatology, 49*, 221–233.

Sofiev, M., Siljamo, P., Ranta, H., Linkosalo, T., Jaeger, S., Jaeger, C., et al. (2012b). From Russia to Iceland: An evaluation of a large-scale pollen and chemical air pollution episode during April and May, 2006. In B. Clot, P. Comtois & B. Escamilla-Garcia (Eds.), *Aerobiological monographs, towards a comprehensive vision*, (Vol. 1, pp. 95–114). MeteoSwiss and University ofMontreal.

Sofiev, M., Siljamo, P., Ranta, H., & Rantio-Lehtimaki, A. (2006a). Towards numerical forecasting of long-range air transport of birch pollen: Theoretical considerations and a feasibility study. *International Journal of Biometeorology, 50*, 392–402.

Sofiev, M., Siljamo, P., Valkama, I., Ilvonen, M., & Kukkonen, J. (2006b). A dispersion modelling system SILAM and its evaluation against ETEX data. *Atmospheric Environment, 40*, 674–685.

Stach, A., Smith, M., SkjØth, C., & Brandt, J. (2007). Examining *Ambrosia* pollen episodes at Poznan (Poland) using back-trajectory analysis. *International Journal of Biometeorology, 51*, 275–286.

Van de Water, P. K., Keever, T., Main, C. E., & Levetin, E. (2003). An assessment of predictive forecasting of *Juniperus ashei* pollen movement in the Southern Great Plains, USA. *International Journal of Biometeorology, 48*, 74–82.

Van de Water, P. K., & Levetin, E. (2001). Contribution of upwind pollen sources to the characterization of *Juniperus ashei* phenology. *Grana, 40*, 133–141.

Van de Water, P. K., Watrud, L. S., Lee, E. H., Burdick, C., & King, G. A. (2007). Long-distance GM pollen movement of creeping bentgrass using modeled wind trajectory analysis. *Ecological Applications, 17*, 1244–1256.

Veriankaite, L., Siljamo, P., Sofiev, M., Sauliene, I., & Kukkonen, J. (2010). Modelling analysis of source regions of long-range transported birch pollen that influences allergenic seasons in Lithuania. *Aerobiologia, 26*, 47–62.